

Research Article

Peng Zhang, Cong Wang, Zhenhui Guo, Jian Hong, and Fei Wang*

Effect of polyvinyl alcohol fibers on mechanical properties of nano-SiO₂-reinforced geopolymers under a complex environment

<https://doi.org/10.1515/ntrev-2023-0142>

received April 23, 2023; accepted September 29, 2023

Abstract: Buildings in service are severely affected by the complex environment with multiple coupled factors such as high temperatures, humidity, and inorganic salt attack. In this work, the mechanical properties of nano-SiO₂-reinforced geopolymers (NSGPC) incorporated with varying dosages of polyvinyl alcohol (PVA) fibers were investigated under a complex environment. A simulated environmental chamber was employed to simulate the complex environment with relative humidity, temperature, and NaCl solution concentration of 100%, 45°C, and 5%, respectively. Fly ash/metakaolin geopolymers (GPCs) were fabricated by utilizing 1.5% nano-SiO₂ by weight and five various dosages of PVA fibers by volume (0, 0.2, 0.4, 0.6, and 0.8%). The compressive strength, tensile strength, elastic modulus, and impact resistance of NSGPC eroded in a simulated environmental chamber for 60 days were determined. Then, the impact of the PVA fiber dosage on the mechanical properties of NSGPC under complex environments was analyzed. In addition, scanning electron microscopy (SEM) was employed to evaluate and analyze the microstructural behavior of NSGPC under complex environments. Results indicated that the compressive strength, tensile strength, elastic modulus, and impact resistance of NSGPC increased with increasing PVA fiber to 0.6% and then decreased with a continuous increase to 0.8% but remained higher than those of the reference specimen. NSGPC exhibited the best performance at a PVA fiber dosage of 0.6%, which increased by 13.3, 12.0, 17.2, and 522%, respectively. The outcomes of SEM analysis

indicated that the usage of PVA fiber and NS remarkably improved the mechanical properties and microstructural behavior of GPC by making the inner structure of GPCs more robust and compact under a complex environment. The outcomes of this work can provide theoretical guidance for buildings serving under a complex environment.

Keywords: geopolymers, composite, polyvinyl alcohol fiber, nano-SiO₂, mechanical properties, complex environment, microstructural behavior

1 Introduction

As urbanization and industrialization further develop, cement is widely used in the construction field due to its excellent mechanical performance and low price. Nevertheless, during the mass production of cement, large dosages of toxic and harmful greenhouse gases are produced, which has a very serious impact on the ecological environment and human society [1–3]. Recent studies indicate that the annual global consumption of concrete is about 40 billion tons and CO₂ emissions are about 10% of the total global CO₂ emissions [4–6]. Hence, it is imperative to search for a low-carbon, environmentally friendly, green, and reliable material that can replace ordinary cement for reducing CO₂ emissions and global sustainable development in the construction and industrial sectors.

Geopolymer has drawn considerable attention from researchers in recent decades owing to its excellent properties in compression strength and impact resistance [7–10]. It is usually made from industrial by-products rich in silicium-aluminates or natural raw materials (*i.e.*, metakaolin [MK], fly ash [FA], blast furnace slag, *etc.*) activated with alkali solutions (NaOH, Na₂CO₃, or Na₂SiO₃, *etc.*). During the mixing process, the silicon–aluminum bond is broken in the alkaline environment, and then the free silicate ions and [AlO₄]⁴⁻ undergo a condensation reaction to form Si–O–Al bonds, resulting in a stable three-dimensional net-like structure. Many studies have revealed that geopolymers have high early strength, high densification,

* Corresponding author: Fei Wang, Yellow River Laboratory, Zhengzhou University, Zhengzhou, 450001, China, e-mail: wangfei0826@163.com

Peng Zhang, Cong Wang: Yellow River Laboratory, Zhengzhou University, Zhengzhou, 450001, China

Zhenhui Guo, Jian Hong: China Construction Seventh Engineering Division Co., Ltd., Zhengzhou, 450004, China

and excellent erosion resistance [11,12]. However, similar to concrete, geopolymers, as a brittle material, has many disadvantages such as low tensile strength and poor toughness, which limit its application in practical projects with relatively high requirements for strength.

A variety of approaches have been employed to compensate for the lack of performance of the geopolymers composite (GPC). Among them, the utilization of nanoparticles (NPs) to enhance the properties of GPC is one of the most common methods used by researchers. The commonly employed nanomaterials include nano-SiO₂ (NS), nano-TiO₂, nano-CaCO₃, and nano-Al₂O₃. Many reports have demonstrated that using a certain dosage of NPs instead of raw materials in concrete is convincing for enhancing the performance of the concrete composite [1,13–15]. Due to the unique properties of NPs in terms of small size effect, and surface effect, after being incorporated into GPC, NPs can fill in the tiny pores in GPC and improve its internal structure [16]. Also, NPs can be used as reactants to enhance the polymerization reaction and improve the interfacial bonding behavior of cementitious materials and aggregates [17].

Related research results indicate that the addition of fibers can improve the mechanical performance of GPCs, and enhance cracking resistance and toughness of GPCs [18–21]. The fibers commonly blended in the GPC matrix are steel fibers [22–24], polyvinyl alcohol (PVA) fibers [25,26], basalt fibers [27], polyethylene fibers [28], *etc.* Among them, the PVA fiber is an excellent choice to strengthen the toughness of GPCs owing to its good hydrophilicity, high toughness, green environment, and excellent acid and alkaline resistance [29–32]. When the PVA fiber is incorporated into the GPC, the uniform distribution of fibers in the matrix can bear part of the external force, effectively reducing the weak areas in the inner structure of the GPC, also limiting its plastic deformation, reducing the number of cracks, and delaying the evolution of cracks [18,33]. Hence, PVA fiber is widely utilized as a reinforcement material in the field of construction for the preparation of PVA fiber-reinforced GPCs. It has been shown that the mechanical properties of GPCs with an appropriate dosage of PVA fibers were remarkably higher than those of the reference specimens without PVA fibers [34].

Greenhouse gas is making the external environment more complex. In such a complex environment, buildings

in service, especially those in coastal areas, are most severely affected by multiple coupled factors (*i.e.*, high temperatures, humidity, high salt concentration, *etc.*). Inorganic ions (*e.g.*, Cl[−], SO₄^{2−}) in seawater erode the inner structure of buildings by diffusion and osmosis [35–37]. Water in the humid environment acts as a carrier for the diffusion of inorganic ions in the matrix, facilitating the erosion action. High temperatures can cause water molecules and inorganic ions to become more active, so that the rate of penetration increases, thereby accelerating the corrosion effect [38]. Thus, the study of the strengthening method and strengthening mechanism of the specimen strength and toughness under a complex environment can be of great help for the engineering application in a complex coupled environment.

Though there are many studies on the performance of nano-SiO₂ or PVA fiber-reinforced GPCs, studies on the use of nano-SiO₂ in conjunction with PVA fibers in GPC under complex environments are still inadequate. This work aims to investigate the influence of PVA fiber dosage (by volume) on the mechanical properties of nano-SiO₂-reinforced geopolymers (NSGPC) under complex environments. The compressive strength, tensile strength, elastic modulus, and impact resistance of NSGPC specimens after 60 days of erosion in a simulated environmental chamber were studied and analyzed. The microstructural characteristics of NSGPC were evaluated by scanning electron microscopy (SEM). The outcomes of this work can provide theoretical guidance for buildings serving in complex environments.

2 Experiments

2.1 Materials

The fibers with different properties made of high-quality PVA, shown in Table 1, were used as additives with four varying dosages (0.2, 0.4, 0.6, 0.8% by volume) in GPCs. The appearance of PVA fibers is shown in Figure 1.

In this work, low-calcium FA and MK have been employed as geopolymers precursors. MK is a fine, pink-white, highly reactive mineral admixture with a mean

Table 1: Properties of PVA fibers

Length (mm)	Tensile strength (MPa)	Specific gravity (g/cm ³)	Elongation at fracture (%)
9	1,400	1.32	15



Figure 1: Appearance of PVA fibers.

particle size of 1.26 μm . FA is a fine-gray powdery solid ash with a density of approximately 2.16 g/cm³. The chemical composition of the precursor obtained from the X-ray fluorescence analysis is provided in Table 2.

The alkali activator for preparing GPCs contained Na₂SiO₃ (light-yellow liquid, about 40% solid, modulus: 3.2) and NaOH (pure white flaky solid, 99% purity). The dosage of NS in GPC is 1.5% by weight, which is due to the best mechanical properties of GPC at this dosage [39].

The performance of NS used in this work is given in Table 3.

2.2 Mix proportions and geopolymers synthesis

The proportions of GPCs prepared in this study are shown in Table 4. Five different GPCs were prepared by adding varying dosages of PVA fibers and an equal dosage of NS. The compressive strength, tensile strength, elastic modulus, and impact resistance of each group of GPCs were tested. In this work, the ratio of MK/FA was kept at 1.5, the water/binder ratio was 0.52, the aggregate/binder was considered 3.0, and the modulus of the alkali activator was kept at 1.3 for all samples. All GPCs were made with 1.5% NS (by weight) and PVA fibers (by volume) in dosages of 0.2, 0.4, 0.6, and 0.8%, respectively.

In this study, a 50 L capacity mechanical mixer was employed for mixing in order to obtain a homogeneous and workable paste. First of all, in order to disperse the fibers, PVA fibers were incorporated into the mixtures and stirred for 2 min before the precursor and river sand were added to the alkali-activator solution. Then, the alkali

Table 2: Chemical composition of precursors

Composition (wt%)	SiO ₂	Al ₂ O ₃	Fe ₂ O ₃	MgO + CaO	K ₂ O + Na ₂ O	SO ₃	Other
MK	54.0	43.0	≤1.3	≤0.8	≤0.7	—	≥0.2
FA	60.98	24.47	6.70	5.58	—	0.52	1.75

Table 3: Properties of NS

Content (%)	Specific surface area (m ² /g)	Mean particle size (nm)	pH	Bulk density (g/cm ³)
99.5	200	30	6	0.035

Table 4: Mix design

Mix ID	Precursor (kg/m ³)		Alkali activator (kg/m ³)		Water (kg/m ³)	Coarse aggregate (kg/m ³)	Fine aggregate (kg/m ³)	NS (%)	PVA fibers (%)
	MK	FA	Na ₂ SiO ₃	NaOH					
C	273	195	286	53.2	79	1,072	577	0	0
NP-0.2	269	192	286	53.2	79	1,072	577	1.5	0.2
NP-0.4	269	192	286	53.2	79	1,072	577	1.5	0.4
NP-0.6	269	192	286	53.2	79	1,072	577	1.5	0.6
NP-0.8	269	192	286	53.2	79	1,072	577	1.5	0.8

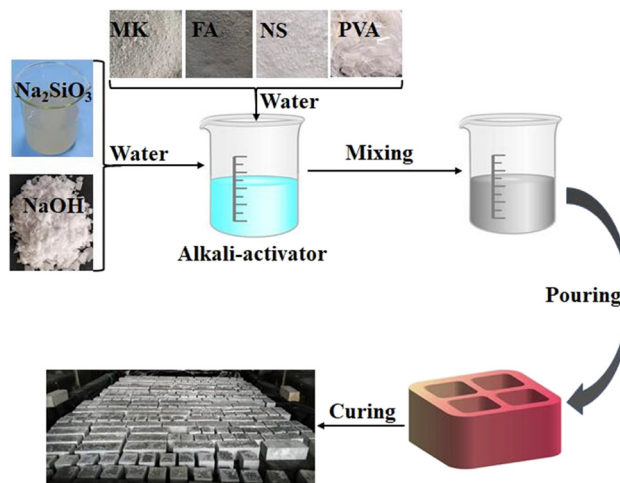


Figure 2: Preparation process of NSGPC.

activator, NS, and water were incorporated into the mix and mixed for 1 min, and subsequently, the graded gravel was added to the mixer and mixed for 2 min. Finally, the prepared GPC paste was poured into different kinds of molds to form the desired specimens. Each GPC specimen was maintained for 28 days at room temperature. Subsequently, the fabricated specimens were placed in an environmental simulation oven to perform a series of mechanical tests. Figure 2 provides the flow chart for fabricating the GPC.

2.3 Environment simulation and test methods

2.3.1 Simulation of the complex environment

With reference to the complex environment of the south-eastern coastal region of China, the effects of three coupled factors, namely humidity, temperature, and chloride salt

erosion, on NSGPC were studied comprehensively. In this work, a simulated environmental test chamber produced by Shanghai Tong Rui Instrument and Equipment Co., Ltd. was employed to simulate the complex environment. Inside the test chamber, heaters and sprayers were adopted to simulate the changes in temperatures and humidity under external conditions. A reservoir was built in the simulated environmental chamber to store NaCl solution at a concentration of 5% for simulating the effect of chloride salt erosion on the specimens. Figure 3 presents the exterior and inner structure of the test chamber.

For the complex environment simulation, the relative humidity, temperature, concentration of the salt solution, and duration of the chamber were kept at 100%, 45°C, 5%, and 60 days, respectively. In addition, in order to simulate the complex outdoor environment more imaginatively and objectively, the dry-wet cycle method was employed in this experiment, *i.e.*, each GPC specimen was dried for 3 days and immersed for 3 days in each cycle. Meanwhile, sprayers were employed to spray NaCl solution or water on the specimen to make the humidity and NaCl concentration meet the test requirements.

2.3.2 Compressive and splitting tensile strength test

A total of 15 cube specimens having sizes of 100 mm × 100 mm × 100 mm were fabricated to perform the compressive strength test of NSGPC according to GB/T50081-2019. A testing machine having a range of 2,000 kN was employed to load the NSGPC specimens at a uniform rate of 0.5 MPa/s until the specimens were damaged. For the objectivity of the results, three specimens were prepared for each proportion, and the mean value of the three NSGPC specimens was set as the compressive strength value of the group for the analysis and discussion of the effect of PVA fiber dosage on compressive strength.



Figure 3: Simulated environmental test chamber. (a) Overall appearance and (b) inner layout.

Fifteen cube samples of NSGPC with sizes of 100 mm × 100 mm × 100 mm were prepared for the tensile strength test. NSGPC specimens were loaded by the test machine at a steady rate of 0.07 MPa/s until the specimens were destroyed. Each ratio consisted of three NSGPC specimens and the mean result was set as the final value for analysis and discussion in this work.

2.3.3 Elastic modulus test

Fifteen prismatic samples of NSGPC with sizes of 300 mm × 100 mm × 100 mm were fabricated to perform the elastic modulus test. The test machine was employed to load and unload the load continuously and uniformly at a rate of 0.5 MPa/s. For each proportion, three specimens were prepared and their mean results were used as the final values. The elastic modulus is obtained by

$$E = \frac{P_a - P_0}{A_3} \times \frac{L}{\Delta n}, \quad (1)$$

where E represents the elastic modulus, P_a represents the load corresponding to the stress of 1/3 axial compressive strength, P_0 represents the load corresponding to 0.5 MPa stress, L represents the measured length, A_3 represents the pressurized area, and Δn represents the mean deformation value of both ends of the sample as the load increases from P_0 to P_a .

2.3.4 Impact resistance test

Similar to previous tests, a total of 25 cube samples of NSGPC with sizes of 100 mm × 100 mm × 100 mm were manufactured to perform the impact resistance test. A drop hammer tester with a 4.5 kg impact hammer was applied to determine the impact toughness of the NSGPC specimens. In detail, the number of impacts corresponding to the first crack in the specimen was defined as the number of initial crack impacts (N_1), the number of impacts corresponding to complete damage was defined as the number of damage impacts (N_2), and the impact toughness was the difference between N_2 and N_1 . Each proportion consisted of five NSGPC specimens, and the mean findings after removing the maximum and minimum values were set as the standard values to ensure the objectivity of the results.

2.3.5 SEM test

In this work, SEM was employed to characterize the cracking characteristics of NSGPC specimens under complex environments.

Before the test, fractured cubic samples with dimensions of 15 mm × 15 mm × 15 mm were placed in a drying oven and dried for 24 h. Subsequently, the NSGPC was sprayed with gold for the microscopic test. The microstructure of the NSGPC specimen was studied by SEM, the micro-morphology was analyzed, and the microform of the NSGPC specimen damage was explored to reveal the mechanism of the influence of the PVA fiber dosage on NSGPC at the microscopic level.

3 Experimental results and discussion

3.1 Compressive strength

The influence of the PVA fiber dosage on the compressive strength of NSGPC under the complex environment is depicted in Figure 4. The compressive strength of the reference GPC specimen under the complex environment is 37.32 MPa. The results indicated that an increase in the PVA fiber dosage to 0.6% led to an increase in the compressive strength of NSGPC, whereas the continuous increase of PVA fiber content to 0.8% caused a decrease in the compressive strength but still greater than the compressive strength of the reference GPC specimens. The compressive strengths of NSGPC specimens dosed with PVA fibers of 0.2% (NSGPC-0.2% PVA), 0.4% (NSGPC-0.4% PVA), and 0.6% (NSGPC-0.6% PVA) by volume enhanced by 10.2, 12.0, and

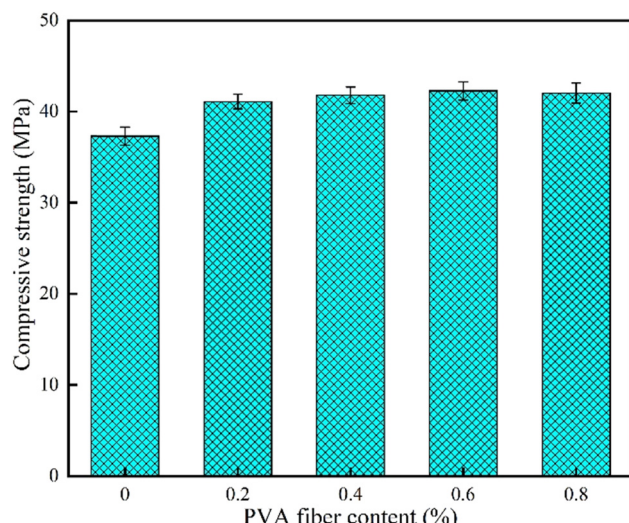


Figure 4: Effect of the PVA fiber dosage on the compressive strength of NSGPC.

13.3%, respectively, compared with the reference specimens under the complex environment. Similarly, Yuan *et al.* [40] revealed that the compressive strength of the geopolymer concrete blended with 50% slag with 0.3% PVA fibers under a complex environment was 14.7% higher than that of the reference specimen. This can be attributed to the fact that the PVA fibers are uniformly dispersed in the NSGPC and inhibit crack initiation and crack propagation by a bridging effect [41–43]. Yet, the compressive strength of the specimens was only 12.6% higher than that of the reference NSGPC specimens when the dosage of PVA fibers was 0.8%, but it was still higher than that of the reference specimens under the complex environment. This may be the result of excessive PVA fiber aggregation inside the matrix destroying the dense, strong internal structure of NSGPC.

From the findings of a previous study, it was evident that the compressive strength of GPC specimens mixed with NS was all higher than that of GPC specimens without NS [44]. This strongly demonstrates the advantage of incorporating 1.5% NS and varying dosages of PVA fibers in the GPC specimens. The enhancement of the compressive strength of GPC specimens with NS can be attributed to the homogeneous dispersion of NS in the matrix, which participates in the polymerization reaction and produces a large dosage of N–A–S–H gels resulting in a compact internal structure of GPC [39,45]. Therefore, it can be concluded that the addition of an appropriate content of PVA fibers and NS into the matrix can enhance the compressive strength of GPC specimens under a complex environment.

3.2 Splitting tensile strength

The influence of the PVA fiber dosage on the tensile strength of NSGPC specimens with 1.5% NS under the complex environment is shown in Figure 5. The findings indicated that the addition of PVA fibers had a certain degree of impact on the tensile strength of NSGPC under the complex environment. Specifically, the tensile strength of the NSGPC specimens having different contents of PVA fibers was higher than that of the reference specimens, and the NSGPC mixed with 0.6% PVA fibers obtained the highest tensile strength, which was 1.12 times higher than that of reference GPC specimens under the complex environment. Notably, Wang *et al.* [46] and Wang *et al.* [47] also discovered that incorporating a certain dosage of fibers in GPCs under complex environments can dramatically improve the tensile strength of NSGPC. Enhancement in tensile strength of NSGPC may be related to the dispersion of PVA fibers in the matrix of the specimen [48,49]. However,

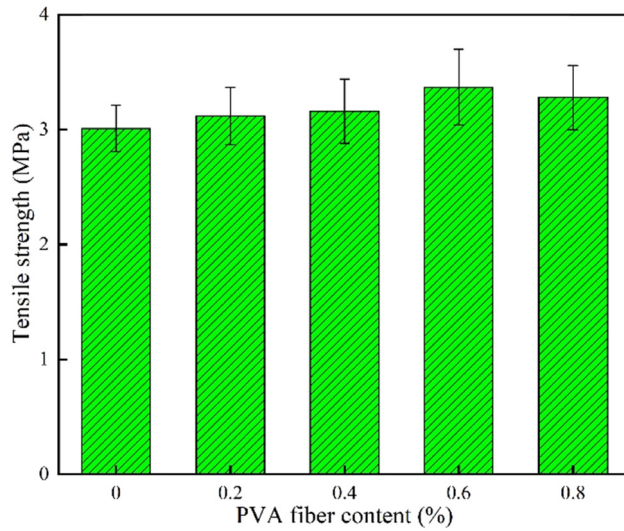


Figure 5: Effect of PVA fiber dosage on the tensile strength of NSGPC.

when the dosage of PVA fibers was 0.8%, the splitting tensile strength of the specimen was only 9% higher than that of the reference NSGPC specimen, but still higher than that of the reference specimen under the complex environment. This may be due to the excessive aggregation of PVA fibers that damaged the dense and strong internal structure of NSGPC.

Similar to the enhancement of the compressive strength, the tensile strength of NSGPC containing different dosages of PVA fibers had a similar effect. In a previous study, the maximum tensile strength of the specimen was 1.95 MPa when 0.6% PVA fibers were added to the geopolymer without NS at high temperatures [50]. Similarly, the maximum compressive strength was 3.37 MPa with 0.6% of PVA fibers in this study, which was much greater than the previous results. Interestingly, the use of PVA fibers along with NS was more beneficial in improving the tensile strength of GPC compared to the reference specimen under the complex environment.

3.3 Elastic modulus

The elastic modulus is one of the crucial factors in evaluating the performance of engineering materials. Specifically, from a macroscopic perspective, the elastic modulus is a measurement of the capacity of a mixture to resist deformation, while from a microscopic perspective, it is a response to the strength of the bonds between molecules and atoms within the structure. Hence, it is vital to analyze and discuss the effect of the dosage of PVA fibers on the elastic moduli of NSGPC and its mechanism under the complex environment. Figure 6 exhibits the influence of PVA fiber dosage on the

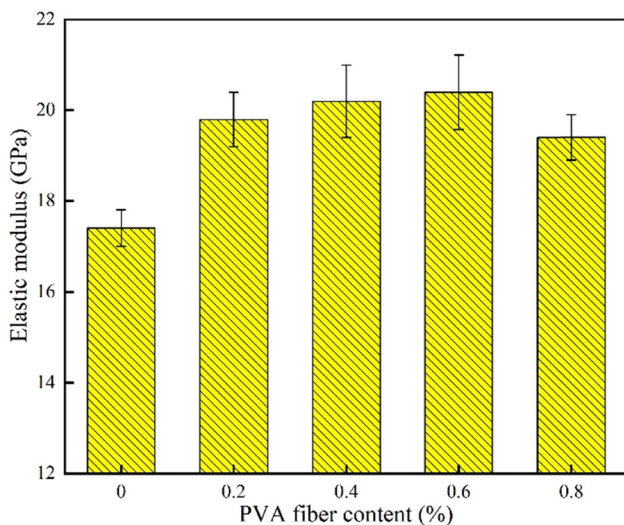


Figure 6: Effect of PVA fiber dosage on the elastic modulus of NSGPC.

elastic moduli of GPC blended with 1.5% NS under the complex environment. The PVA fiber dosage has a remarkable impact on the modulus of elasticity of NSGPC under a complex environment. In detail, the increase in the PVA fiber dosage to 0.6% resulted in an improvement in the elastic modulus of the GPC specimens, while the continuous increase in the PVA fiber dosage to 0.8% led to a decrease in the elastic modulus but still higher than that of the reference specimens. With a PVA fiber dosage of 0.6%, the maximum elastic modulus of 20.2 GPa was obtained for NSGPC, which was 17.2% higher than that of the reference GPC under the complex environment. Incorporating 1.5% NS along with 0.6% PVA fiber in GPC can substantially improve the deformation resistance of GPC under a complex environment.

The enhancement mechanism of the elastic modulus of NSGPC incorporating varied contents of PVA fibers is the same as that of the compressive and tensile strength of NSGPC under a complex environment. When the dosage of PVA fibers in the GPC matrix is less than 0.6%, the PVA fibers can be uniformly dispersed around the interfacial transition zone of NSGPC. Due to the excellent tensile properties of PVA fibers, the ability of GPC to resist deformation can be greatly increased when subjected to external loads. Meanwhile, NS with a mass fraction of 1.5% can be involved in the polymerization reaction to yield considerable N—A—S—H or C—A—S—H, which can improve the microstructure of GPC and play a synergistic effect with PVA fibers [34,51]. Yet, once the dosage of PVA fibers exceeds 0.6%, the excess PVA fibers agglomerate inside the matrix, causing an increasing number of pores in the GPC matrix, which leads to a reduced synergistic effect. However, the negative effect of excess PVA fibers on the elastic moduli of GPCs is weakened due to the presence of NS inside the matrix [52]. This is the reason why the elastic

modulus of NSGPC with 0.8% PVA fiber is still higher than that of the reference GPC under the complex environment.

3.4 Impact resistance

Impact toughness refers to the ability of the material to resist plastic deformation and fracture damage under impact loads, which reflects the internal defects and impact resistance of the material to a certain extent. In this work, the difference between the number of damage impacts (N_2) and the number of initial fracture impacts (N_1) was adopted as the index of NSGPC impact toughness. Figure 7 demonstrates the influence of PVA fiber dosage on the impact resistance of NSGPC under a complex environment. The findings revealed that the impact toughness of GPC under the complex environment increased as the PVA fiber dosage increased to 0.6%, and decreased with the continuous increase to 0.8%. That is, NSGPC incorporated with 0.6% PVA fiber exhibited the maximum impact toughness of 18.67 times, which was 6.22 times higher than that of the reference GPC under the complex environment. Similar outcomes for fiber-reinforced impact resistance have also been reported elsewhere [53,54]. In addition, in this work, note that the impact toughness of all NSGPCs with PVA fibers was greater than that of the reference GPC. It can be deduced that incorporating a certain dosage of PVA fibers in NSGPC could effectively enhance the impact resistance of the specimens under the complex environment.

The enhanced impact toughness of NSGPC with a small dosage of PVA fibers (less than 0.6%) can be ascribed to

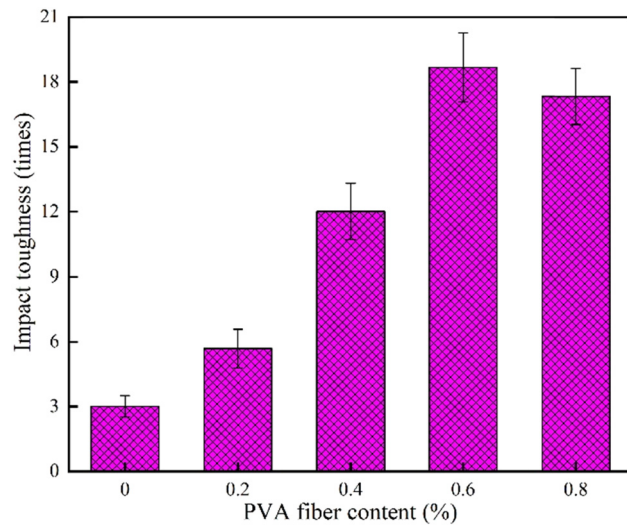


Figure 7: Effect of PVA fiber dosage on the impact resistance of NSGPC.

the association formed between the PVA fiber and the surrounding matrix, leading to an improvement in the ability of the GPC to resist deformation. The bridging effect of PVA fibers improved the structure of the matrix, and limited crack initiation and propagation, which caused an enhancement in the impact toughness of NSGPC under the complex environment. Besides, owing to the excellent properties of NS, NS can effectively fill in the cracks between PVA fibers and the matrix and the micropores inside the matrix, making the structure of GPC much denser and stronger [55,56].

3.5 Relationship between compressive and tensile strength

In previous studies, it was found that there was a correlation between the tensile (f_t) and compressive strength (f_c) of concrete or geopolymers [57,58]. Various fitting models, e.g. linear function fitting model, quadratic function fitting model, and logarithmic function fitting model, were employed to reveal the relationship between f_t and f_c based on the experimental findings [58–61]. In this work, a quadratic function fitting model was employed to characterize the relationship between f_t and f_c of GPC. The fitted curve of f_t versus f_c for NSGPC blended with 0.2, 0.4, 0.6, and 0.8% PVA fibers based on the experimental outcomes is illustrated in Figure 8. Equation (2) exhibits the equation used to fit the f_t and f_c of NSGPC containing varying dosages of PVA fibers. It can be observed that there is a strong relationship between f_t and f_c for NSGPC containing various contents of PVA fibers:

$$f_t = 0.115f_c^2 - 9.34f_c + 192.99, \quad (2)$$

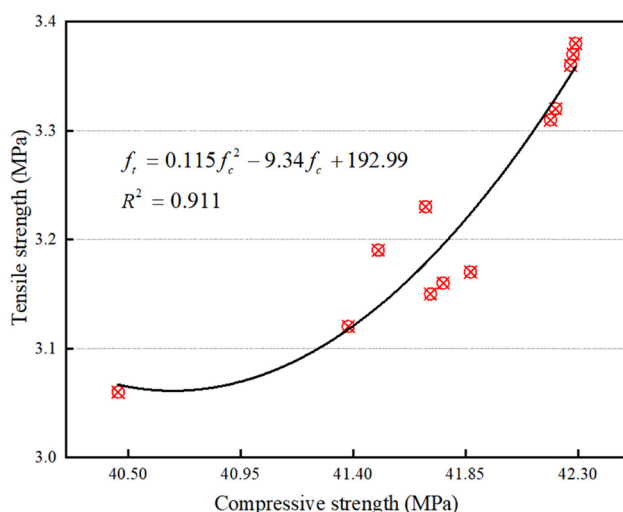


Figure 8: Relationship between tensile and compressive strength of NSGPC containing various dosages of PVA fibers.

where f_t represents the tensile strength and f_c represents the compressive strength.

In the fitting process, the correlation coefficient (R^2) is employed to evaluate the merit of the fitted equation with respect to the experimental outcomes. When R^2 of the fitted equation is around 1, the fitting function is considered reliable. It is acceptable when the R^2 of the fitted function is above 0.9. In this investigation, the R^2 of the GPC fitting equation is 0.911; thus, it can be assumed that the fitting function obtained based on the experimental findings can reflect the relationship between f_t and f_c of GPC to some extent. The results of this study are similar to those of Sofi *et al.* [62], where the f_t and f_c of GPC are enhanced to some extent compared to the strength of the reference specimens. This can be attributed to the involvement of NS in the polymerization reaction in an alkaline environment, which produces a sufficient dosage of gels to form a dense structure and the bridging mechanism of PVA fibers in the interfacial transition zone [63,64].

3.6 Microstructural behavior

The microstructural images of NSGPC blended with varying dosages of PVA fibers under the complex environment are depicted in Figure 9. As shown in the SEM micrographs of GPC, the damage behavior of NSGPC and its strength enhancement mechanism could be clearly understood and analyzed under the complex environment. It can be noted clearly that the microstructure of the reference GPC is remarkably dissimilar to that of the NSGPC with various dosages of PVA fibers. Specifically, in the SEM images of the reference GPC (Figure 9a and b), it is found that the inner structure of the GPC is relatively loose and that numerous cracks and pores appear on the fracture surface, along with a large variety of chloride crystals and corrosion products around the cracks and pores. In contrast, a significant improvement in the internal microstructure of the specimens is observed in NSGPC prepared with 0.6% PVA fibers (Figure 9c and d). In the NSGPC matrix, NS as a filler filled inside the cracks and voids is capable of significantly reducing the porosity of the internal structure and making the structure of the GPC matrix stronger and more compact, thus inhibiting the erosion of the specimens by chlorides as well as various salts [65,66].

Similarly, the microstructural images demonstrate that the PVA fibers are capable of binding effectively to the matrix, which may be related to the particular performance of NS (i.e., small size, large specific surface area, and strong adsorption capacity). As found by Zhang *et al.* [36], the PVA fibers cross over the cracks and prevent the cracks from propagating to the surrounding area. When the applied

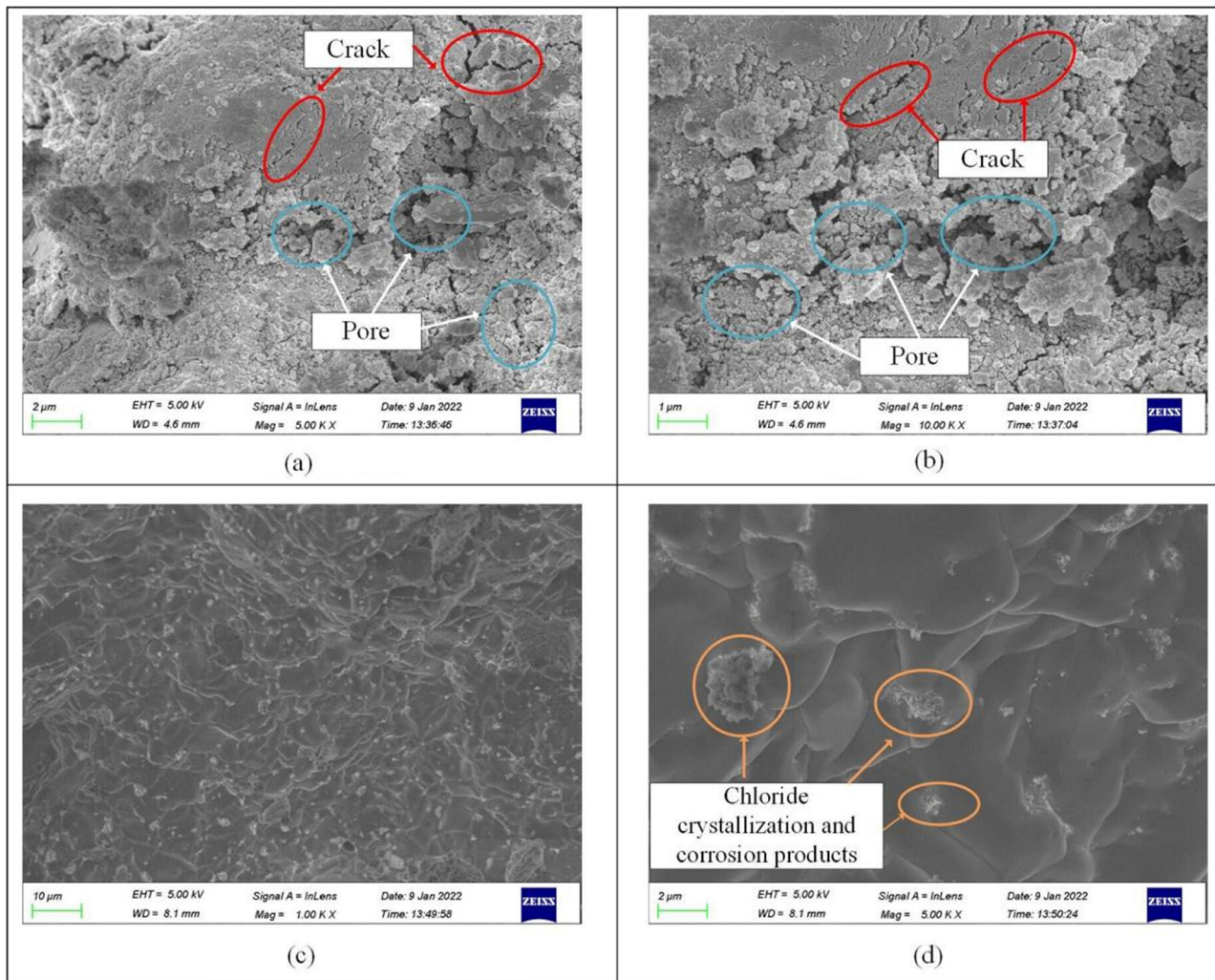


Figure 9: SEM image of GPC. (a and b) Reference GPC, (c and d) NSGPC-0.6%PVA.

external load exceeds a certain threshold value, the weak tensile strength of the PVA fiber and the smooth surface properties cause the PVA fibers to be pulled off or pulled out. Moreover, as the dosages of PVA fibers are too high, the agglomeration and interlacing effect of PVA fibers leads to a considerable number of pores and cracks in the inner structure of GPCs, thus reducing the erosion resistance of GPCs. Nevertheless, owing to the presence of NS, the negative effects of excessive PVA fibers can be weakened to some extent [34,67].

3.7 Mechanisms of effects for complex coupled environments

GPC, as a multi-component composite material, has many micro-cracks and pores inside the structure (Figure 9a and b).

In a complex environment of humidity, high temperatures, and high salt concentration, inorganic salt ions erode the surface of the specimen by diffusion and osmosis. The water molecules in the humid environment act as a carrier for the diffusion of inorganic salt ions in the matrix. High temperatures can both increase the solubility of inorganic salt ions in water and make inorganic salt ions and water molecules more active. Due to the erosion of inorganic salts, the dissolution of water, and the acceleration of temperature, the existing cracks and pores inside the GPC are further developed, and more new cracks and pores are created [35,38,39,68–70]. With the superposition of the coupling effect, the damage to the specimen goes from the surface to the interior.

Figure 10(a)–(d) illustrates the appearance of GPC in the natural environment and complex environment, respectively. It can be found that the appearance of the GPC

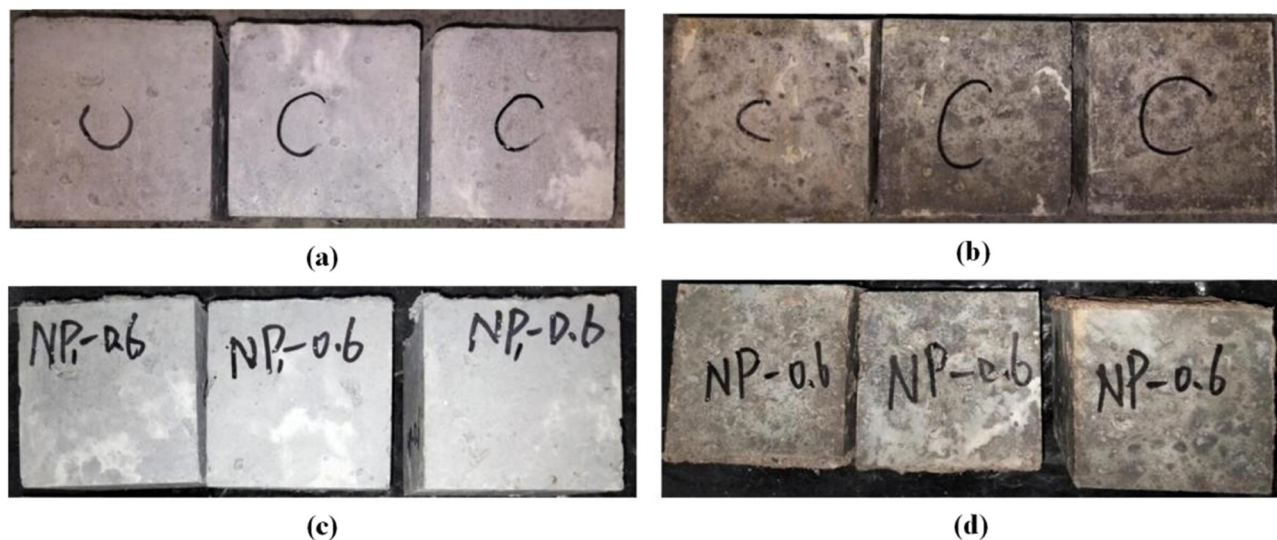


Figure 10: Appearance of GPC in the natural environment and complex environment. (a) Control GPC in the natural environment; (b) control GPC in the complex environments; (c) NSGPC-0.6%PVA in the natural environment; and (d) NSGPC-0.6%PVA in the complex environment.

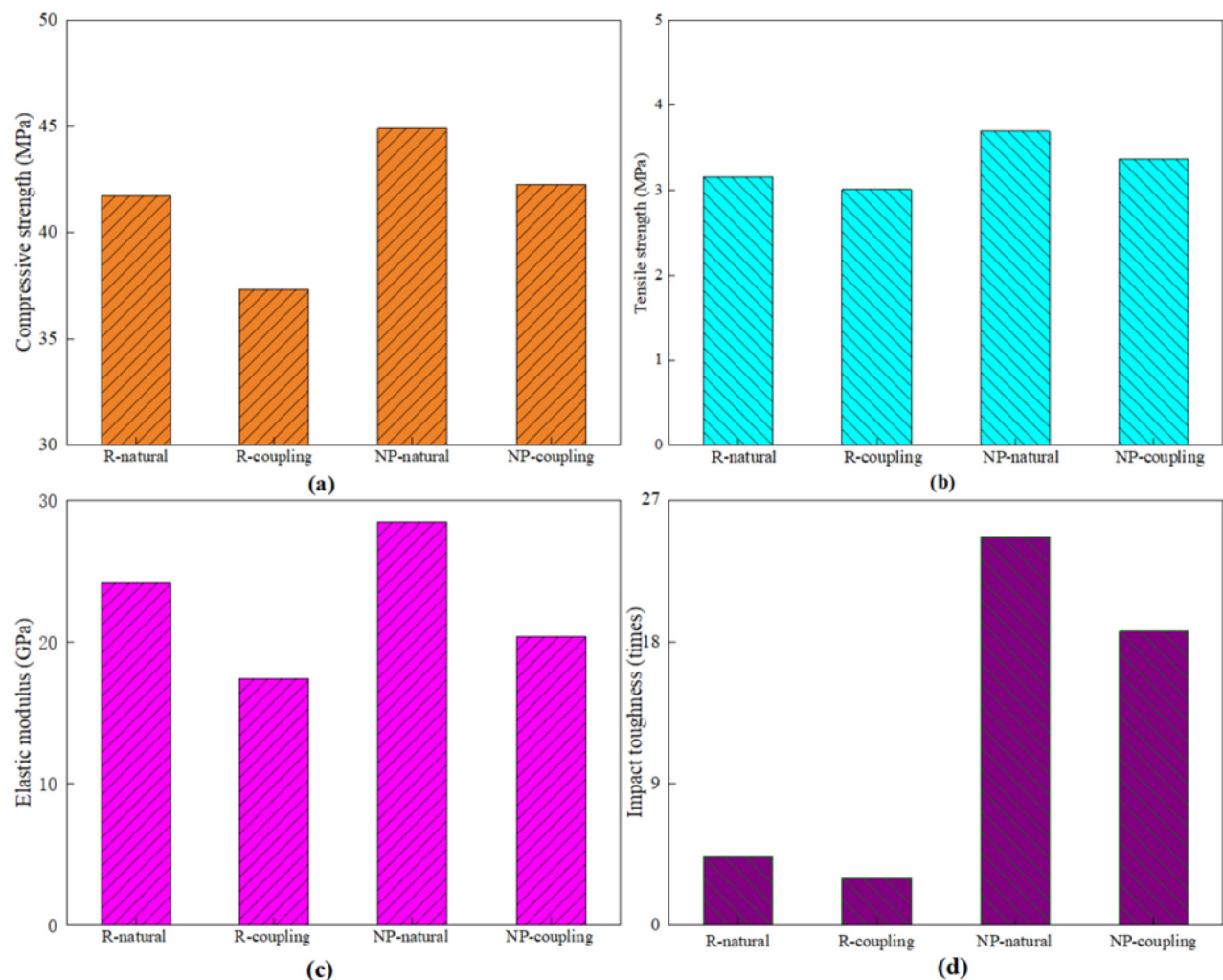


Figure 11: Varying mechanical performances of NSGPC in natural and complex environments. (a) Compressive strength, (b) tensile strength, (c) elastic modulus, and (d) impact toughness.

specimens in the complex environment is considerably different from that under the natural environment. Specifically, the surface of GPCs in the natural environment appeared light gray, whereas the surface of the GPC in the complex environment appeared dark gray and was accompanied by visible pores, inorganic salt crystals, and corrosion products. Among them, the area of surface patches of GPC incorporated with NS and PVA fibers in the complex environment was smaller than that of the surface patches of the reference GPC.

The mechanical behaviors of GPC in natural and complex environments are depicted in Figure 11. In this work, R-natural and R-coupling represent reference GPC specimens under natural and complex environments, respectively; and NP-natural and NP-coupling represent GPC specimens containing 0.6% PVA fiber and 1.5% NS under natural and complex environments, respectively. It can be realized that the mechanical performance of GPC containing PVA fibers and NS is generally higher than the mechanical performance of the corresponding reference specimens, both in natural and complex environments. In addition, it was found that the compressive strength, tensile strength, elastic module, and impact resistance of specimens containing no PVA fiber and NS under complex environments were 10.61, 4.44, 27.98, and 30.72% lower than those of the reference GPC under natural environments, respectively. The compressive strength, tensile strength, elastic module, and impact resistance of specimens containing 0.6% PVA fibers and 1.5% NS in complex environments were 5.81, 8.67, 28.30, and 24.32% lower than those of the corresponding GPC, respectively. This implied that the usage of NS and PVA fiber under a complex environment had an inhibiting impact on the decrease of compressive strength and impact resistance of GPC, while it did not have a remarkable impact on the decrease of tensile strength and elastic module of GPCs. Nevertheless, on the whole, the use of PVA fibers along with NS in GPCs remarkably improved the mechanical performance of GPC under complex environments.

4 Conclusions and further work

This work focuses on the mechanical properties of NSGPC under complex environments reinforced by various contents of PVA fibers. The main conclusions obtained are the following.

1) The compressive strength, tensile strength, and elastic modulus of GPCs blended with 1.5% NS (by weight) initially improved and then reduced with the dosage of PVA fibers (by volume) varying from 0.2 to 0.8% but remained higher than those of the reference specimens under the complex environment. NSGPC with 0.6% PVA fiber yielded the maximum compressive and tensile

strength, and elastic modulus, which were 13.3, 12.0, and 17.2% higher than those of the reference specimen, respectively.

- 2) The impact toughness of NSGPC was first enhanced and then reduced with the PVA fiber dosage in the range of 0.2–0.8% but was still higher than that of the reference specimen under the complex environment. The highest impact resistance was also achieved for NSGPC with 0.6% PVA fiber, which was 6.22 times higher than that of the reference specimen.
- 3) The enhancement in strength and erosion resistance of the GPC under the complex environment was due to the PVA fibers incorporated in the NSGPC matrix limiting crack generation and propagation through the bridging effect. PVA fibers could effectively bind to the matrix, owing to the NS improving and providing a stronger and more compact inner structure of the GPC.

Buildings in service are not only subjected to temperatures, humidity, and chloride attack but also subjected to long-term loads and variable loads. Under the complex environment, long-term loads or variable loads cause varying degrees of damage to geopolymer concrete structures. Therefore, it is important to further investigate the long-term performance (such as impermeability, frost resistance, and chloride erosion resistance) of geopolymer concrete under a complex environment.

Funding information: The authors would like to acknowledge the financial support received from the National Natural Science Foundation of China (Grant No. 5227283, U2040224), Natural Science Foundation of Henan (Grant No. 212300410018), and Project Special Funding of Yellow River Laboratory (Grant No. YRL22LT02).

Author contributions: All authors have accepted responsibility for the entire content of this manuscript and approved its submission.

Conflict of interest: The authors state no conflict of interest.

References

- [1] Alomayri T, Raza A, Shaikh F. Effect of nano SiO₂ on mechanical properties of micro-steel fibers reinforced geopolymers composites. *Ceram Int*. 2021;47(23):33444–53.
- [2] Han X, Zhang P, Zheng Y, Wang J. Utilization of municipal solid waste incineration fly ash with coal fly ash/metakaolin for geopolymers preparation. *Constr Build Mater*. 2023;403:133060.

[3] Zhang P, Wang C, Wang F, Yuan P. Influence of sodium silicate to precursor ratio on mechanical properties and durability of the metakaolin/fly ash alkali-activated sustainable mortar using manufactured sand. *Rev Adv Mater Sci.* 2023;62(1):20220310.

[4] Zhang CY, Han R, Yu BY, Wei YM. Accounting process-related CO₂ emissions from global cement production under shared socioeconomic pathways. *J Clean Prod.* 2018;184:451–65.

[5] Van Damme H. Concrete material science: Past, present, and future innovations. *Cem Concr Res.* 2018;112:5–24.

[6] Zhang P, Su J, Guo J, Hu S. Influence of carbon nanotube on properties of concrete: A review. *Constr Build Mater.* 2023;369:130388.

[7] Tang Z, Li W, Tam VWY, Luo Z. Investigation on dynamic mechanical properties of fly ash/slag-based geopolymers recycled aggregate concrete. *Compos Part B-Eng.* 2020;185:107776.

[8] Kong DLY, Sanjayan JG. Damage behavior of geopolymer composites exposed to elevated temperatures. *Cem Concr Compos.* 2008;30(10):986–91.

[9] Chan CL, Zhang MZ. Behaviour of strain hardening geopolymers composites at elevated temperatures. *Cem Concr Compos.* 2022;132:104634.

[10] Nis A, Eren NA, Cevik A. Effects of recycled tyre rubber and steel fibre on the impact resistance of slag-based self-compacting alkali-activated concrete. *Eur J Environ Civ Eng.* 2023;27(1):519–37.

[11] Zhang ZM, Chen R, Hu J, Wang YY, Huang HL, Ma YW, et al. Corrosion behavior of the reinforcement in chloride-contaminated alkali-activated fly ash pore solution. *Compos Part B-Eng.* 2021;224:109215.

[12] Behera P, Baheti V, Militky J, Naeem S. Microstructure and mechanical properties of carbon microfiber reinforced geopolymers at elevated temperatures. *Constr Build Mater.* 2018;160:733–43.

[13] Zhang P, Wang MH, Han X, Zheng YX. A review on properties of cement-based composites doped with graphene. *J Build Eng.* 2023;70:106367.

[14] Zhang P, Sun YW, Wei JD, Zhang TH. Research progress on properties of cement-based composites incorporating graphene oxide. *Rev Adv Mater Sci.* 2023;62(1):20220329.

[15] Nis A, Eren NA, Cevik A. Effects of nanosilica and steel fibers on the impact resistance of slag based self-compacting alkali-activated concrete. *Ceram Int.* 2021;47(17):23905–18.

[16] Wang C, Zhang P, Guo JJ, Wang J, Zhang TH. Durability and microstructure of cementitious composites under the complex environment: Synergistic effects of nano-SiO₂ and polyvinyl alcohol fiber. *Constr Build Mater.* 2023;400:132621.

[17] Phoo-ngernkham T, Chindaprasirt P, Sata V, Hanjitsuwan S, Hatanaka S. The effect of adding nano-SiO₂ and nano-Al₂O₃ on properties of high calcium fly ash geopolymers cured at ambient temperature. *Mater Des.* 2014;55:58–65.

[18] Zhang P, Han X, Hu SW, Wang J, Wang TY. High-temperature behavior of polyvinyl alcohol fiber-reinforced metakaolin/fly ash-based geopolymers mortar. *Compos Part B-Eng.* 2022;244:110171.

[19] Tanyildizi H, Yonar Y. Mechanical properties of geopolymers concrete containing polyvinyl alcohol fiber exposed to high temperature. *Constr Build Mater.* 2016;126:381–7.

[20] Shirai K, Horii J, Nakamura K, Teo W. Experimental investigation on the mechanical and interfacial properties of fiber-reinforced geopolymers layer on the tension zone of normal concrete. *Constr Build Mater.* 2022;360:129568.

[21] Zhang P, Wei SY, Wu JJ, Zhang Y, Zheng YX. Investigation of mechanical properties of PVA fiber-reinforced cementitious composites under the coupling effect of wet-thermal and chloride salt environment. *Case Stud Constr Mater.* 2022;17:e01325.

[22] Zhang P, Wang C, Gao Z, Wang F. A review on fracture properties of steel fiber reinforced concrete. *J Build Eng.* 2023;67:105975.

[23] Chen G, Zheng D-P, Chen Y-W, Lin J-X, Lao W-J, Guo Y-C, et al. Development of high performance geopolymers concrete with waste rubber and recycle steel fiber: A study on compressive behavior, carbon emissions and economical performance. *Constr Build Mater.* 2023;393:131988.

[24] Lin JX, Su JY, Pan HS, Peng YQ, Guo YC, Chen WS, et al. Dynamic compression behavior of ultra-high performance concrete with hybrid polyoxymethylene fiber and steel fiber. *J Mater Res Technol-JMRT.* 2022;20:4473–86.

[25] Al-Majidi MH, Lampropoulos AP, Cundy AB, Tsoulou OT, Al-Rekabi S. A novel corrosion resistant repair technique for existing reinforced concrete (RC) elements using polyvinyl alcohol fibre reinforced geopolymers concrete (PVAFRGC). *Constr Build Mater.* 2018;164:603–19.

[26] Lin JX, Song Y, Xie ZH, Guo YC, Yuan B, Zeng JJ, et al. Static and dynamic mechanical behavior of engineered cementitious composites with PP and PVA fibers. *J Build Eng.* 2020;29:101097.

[27] Zheng Y, Zhuo J, Zhang P, Ma M. Mechanical properties and meso-microscopic mechanism of basalt fiber-reinforced recycled aggregate concrete. *J Clean Prod.* 2022;370:133555.

[28] Peng YQ, Zheng DP, Pan HS, Yang JL, Lin JX, Lai HM, et al. Strain hardening geopolymers composites with hybrid POM and UHMWPE fibers: Analysis of static mechanical properties, economic benefits, and environmental impact. *J Build Eng.* 2023;76:107315.

[29] Zhao N, Wang SL, Quan XY, Xu F, Liu KN, Liu Y. Behavior of polyvinyl alcohol fiber reinforced geopolymers composites under the coupled attack of sulfate and freeze-thaw in a marine environment. *Ocean Eng.* 2021;238:109734.

[30] Si W, Cao ML, Li L. Establishment of fiber factor for rheological and mechanical performance of polyvinyl alcohol (PVA) fiber reinforced mortar. *Constr Build Mater.* 2020;265:120347.

[31] Xu F, Deng X, Peng C, Zhu J, Chen JP. Mix design and flexural toughness of PVA fiber reinforced fly ash-geopolymer composites. *Constr Build Mater.* 2017;150:179–89.

[32] Zhang P, Gao Z, Wang J, Guo JJ, Wang TY. Influencing factors analysis and optimized prediction model for rheology and flowability of nano-SiO₂ and PVA fiber reinforced alkali-activated composites. *J Clean Prod.* 2022;366:132988.

[33] Choi JI, Song KI, Song JK, Lee BY. Composite properties of high-strength polyethylene fiber-reinforced cement and cementless composites. *Compos Struct.* 2016;138:116–21.

[34] Wang KX, Zhang P, Guo JJ, Gao Z. Single and synergistic enhancement on durability of geopolymers mortar by polyvinyl alcohol fiber and nano-SiO₂. *J Mater Res Technol-JMRT.* 2021;15:1801–14.

[35] Tang LP. Concentration dependence of diffusion and migration of chloride ions - Part 1. Theoretical considerations. *Cem Concr Res.* 1999;29(9):1463–8.

[36] Zhang P, Yuan P, Guan JF, Guo JJ. Fracture behavior of multi-scale nano-SiO₂ and polyvinyl alcohol fiber reinforced cementitious composites under the complex environments. *Theor Appl Fract Mech.* 2022;122:103584.

[37] Yang CC. On the relationship between pore structure and chloride diffusivity from accelerated chloride migration test in cement-based materials. *Cem Concr Res.* 2006;36(7):1304–11.

[38] Jiang WQ, Shen XH, Xia J, Mao LX, Yang J, Liu QF. A numerical study on chloride diffusion in freeze-thaw affected concrete. *Constr Build Mater.* 2018;179:553–65.

[39] Jin QQ, Zhang P, Wu JJ, Sha DH. Mechanical properties of nano-SiO₂ reinforced geopolymers concrete under the coupling effect of a wet-thermal and chloride salt environment. *Polymers*. 2022;14(11):2298.

[40] Yuan Y, Zhao RD, Li R, Wang YB, Cheng ZQ, Li FH, et al. Frost resistance of fiber-reinforced blended slag and Class F fly ash-based geopolymers concrete under the coupling effect of freeze-thaw cycling and axial compressive loading. *Constr Build Mater*. 2020;250:118831.

[41] Humur G, Cevik A. Effects of hybrid fibers and nanosilica on mechanical and durability properties of lightweight engineered geopolymers composites subjected to cyclic loading and heating-cooling cycles. *Constr Build Mater*. 2022;326:126846.

[42] Zhong H, Zhang MZ. Dynamic splitting tensile behaviour of engineered geopolymers composites with hybrid polyvinyl alcohol and recycled tire polymer fibres. *J Clean Prod*. 2022;379:134779.

[43] Noushini A, Samali B, Vessalas K. Effect of polyvinyl alcohol (PVA) fibre on dynamic and material properties of fibre reinforced concrete. *Constr Build Mater*. 2013;49:374–83.

[44] Cheng ZJ, Lu YY, An JP, Zhang HJ, Li S. Multi-scale reinforcement of multi-walled carbon nanotubes/polyvinyl alcohol fibers on lightweight engineered geopolymers composites. *J Build Eng*. 2022;57:104889.

[45] Xu H, Van Deventer JSJ. The geopolymersation of alumino-silicate minerals. *Int J Miner Process*. 2000;59(3):247–66.

[46] Wang Y, Zhang SH, Niu DT, Fu Q. Quantitative evaluation of the characteristics of air voids and their relationship with the permeability and salt freeze-thaw resistance of hybrid steel-polypropylene fiber-reinforced concrete composites. *Cem Concr Compos*. 2022;125:104292.

[47] Wang L, He TS, Zhou YX, Tang SW, Tan JJ, Liu ZT, et al. The influence of fiber type and length on the cracking resistance, durability and pore structure of face slab concrete. *Constr Build Mater*. 2021;282:122706.

[48] Xu SL, Malik MA, Qi Z, Huang BT, Li QH, Sarkar M. Influence of the PVA fibers and SiO₂ NPs on the structural properties of fly ash based sustainable geopolymers. *Constr Build Mater*. 2018;164:238–45.

[49] Zhang P, Wei SY, Zheng YX, Wang F, Hu SW. Effect of single and synergistic reinforcement of PVA fiber and nano-SiO₂ on workability and compressive strength of geopolymers composites. *Polymers*. 2022;14(18):3765.

[50] Deng ZM, Yang ZF, Bian J, Lin JJ, Long ZS, Hong GZ, et al. Advantages and disadvantages of PVA-fibre-reinforced slag- and fly ash-blended geopolymers composites: Engineering properties and microstructure. *Constr Build Mater*. 2022;349:128690.

[51] Gulsan ME, Alzebaree R, Rasheed AA, Nis A, Kurtoglu AE. Development of fly ash/slag based self-compacting geopolymers concrete using nano-silica and steel fiber. *Constr Build Mater*. 2019;211:271–83.

[52] Zhang P, Wang KX, Wang J, Guo JJ, Ling YF. Macroscopic and microscopic analyses on mechanical performance of metakaolin/fly ash based geopolymers mortar. *J Clean Prod*. 2021;294:126193.

[53] Xiao SH, Liao SJ, Zhong GQ, Guo YC, Lin JX, Xie ZH, et al. Dynamic properties of PVA short fiber reinforced low-calcium fly ash-slag geopolymers under an SHPB impact load. *J Build Eng*. 2021;44:103220.

[54] Li WM, Xu JY. Impact characterization of basalt fiber reinforced geopolymers concrete using a 100-mm-diameter split Hopkinson pressure bar. *Mater Sci Eng A-Struct Mater Prop Microstruct Process*. 2009;513–514:145–53.

[55] Li WG, Long C, Tam VVY, Poon CS, Duan WH. Effects of nanoparticles on failure process and microstructural properties of recycled aggregate concrete. *Constr Build Mater*. 2017;142:42–50.

[56] Shaikh FUA, Shafeei Y, Sarker PK. Effect of nano and micro-silica on bond behaviour of steel and polypropylene fibres in high volume fly ash mortar. *Constr Build Mater*. 2016;115:690–8.

[57] Ryu GS, Lee YB, Koh KT, Chung YS. The mechanical properties of fly ash-based geopolymers concrete with alkaline activators. *Constr Build Mater*. 2013;47:409–18.

[58] Choi Y, Yuan RL. Experimental relationship between splitting tensile strength and compressive strength of GFRC and PFRC. *Cem Concr Res*. 2005;35(8):1587–91.

[59] Zhao SB, Ding XX, Zhao MS, Li CY, Pei SW. Experimental study on tensile strength development of concrete with manufactured sand. *Constr Build Mater*. 2017;138:247–53.

[60] Yildirim H, Ozturan T. Impact resistance of concrete produced with plain and reinforced cold-bonded fly ash aggregates. *J Build Eng*. 2021;42:102875.

[61] Gesoglu M, Guneyisi E, Alzebaree R, Mermerdas K. Effect of silica fume and steel fiber on the mechanical properties of the concretes produced with cold bonded fly ash aggregates. *Constr Build Mater*. 2013;40:982–90.

[62] Sofi M, van Deventer JSJ, Mendis PA, Lukey GC. Engineering properties of inorganic polymer concretes (IPCs). *Cem Concr Res*. 2007;37(2):251–7.

[63] Zanotti C, Borges PHR, Bhutta A, Bonthia N. Bond strength between concrete substrate and metakaolin geopolymers repair mortar: Effect of curing regime and PVA fiber reinforcement. *Cem Concr Compos*. 2017;80:307–16.

[64] Ibrahim M, Johari MAM, Maslehuddin M, Rahman MK. Influence of nano-SiO₂ on the strength and microstructure of natural pozzolan based alkali activated concrete. *Constr Build Mater*. 2018;173:573–85.

[65] Yin SP, Jing L, Yin MT, Wang B. Mechanical properties of textile reinforced concrete under chloride wet-dry and freeze-thaw cycle environments. *Cem Concr Compos*. 2019;96:118–27.

[66] Yip CK, Lukey GC, Provis JL, van Deventer JSJ. Effect of calcium silicate sources on geopolymersation. *Cem Concr Res*. 2008;38(4):554–64.

[67] Escalante-Garcia JI, Sharp JH. The chemical composition and microstructure of hydration products in blended cements. *Cem Concr Compos*. 2004;26(8):967–76.

[68] Ozyurt N, Soylev TA, Ozturan T, Pehlivan AO, Nis A. Corrosion and chloride diffusivity of reinforced concrete cracked under sustained flexure. *Tek Dergi*. 2020;31(6):10315–37.

[69] Niş A, Çevik A. 18-Seawater resistance of alkali-activated concrete. In: Pacheco-Torgal F, Chindaprasirt P, Ozbakkaloglu T, editors. *Handbook of advances in alkali-activated concrete*. Sawston, United Kingdom: Woodhead Publishing; 2022. p. 451–69.

[70] Kurtoglu AE, Alzebaree R, Aljumaili O, Nis A, Gulsan ME, Humur G, et al. Mechanical and durability properties of fly ash and slag based geopolymers concrete. *Adv Concr Constr*. 2018;6(4):345–62.